THE ASTROPHYSICAL JOURNAL SUPPLEMENT SERIES, 56:283–294, 1984 October

SURFACE PHOTOMETRY OF EDGE-ON GALAXIES. V. THE VERTICAL STRUCTURE OF THE BAR IN NGC 4762

KEN-ICHI WAKAMATSU[1]
Physics Department, Junior Technical College, Gifu University, Japan
AND
MASARU HAMABE
Tokyo Astronomical Observatory, University of Tokyo, Japan
Received 1984 January 4; accepted 1984 April 27

ABSTRACT

Surface photometry has been made for the edge-on S0 galaxy NGC 4762. Brightness profiles both parallel and perpendicular to the equatorial plane indicate that the galaxy has four distinct components. We present evidence that these components should be identified as a nuclear bulge, bar, lens, and outer ring. We propose that NGC 4762 is an early-type *barred* galaxy with a bar seen obliquely at an angle $\phi = 33° \pm 10°$ to the line of sight.

The brightness profile is decomposed into its separate components to study the structure of the bar and the lens. The vertical luminosity profiles of the lens decrease less steeply than an isothermal sheet model and can be well fitted to Camm's case II model with $n = 1.0$. The scale height $\bar{z}$ is constant with distance from the galactic center, and $\bar{z} = 560 \pm 40$ pc. The profile of the bar can be fitted to an isothermal model with a scale height $\bar{z} = 155 \pm 15$ pc, i.e., only one-third of that of the lens. The vertical velocity dispersion of the bar is estimated to be about half of that of the lens, which implies that the bar has a different kinematical structure from the lens.

Subject headings: galaxies: individual — galaxies: photometry — galaxies: structure

I. INTRODUCTION

Ordinary and barried spiral galaxies are essentially distinguished from elliptical galaxies by the presence of fundamental planes. Studies of the vertical structure of disks are very important for our understanding of formation and evolution of disks. Van der Kruit and Searle (1981*a*, *b*, 1982*a*, *b*) examined several edge-on spiral galaxies and obtained the following results: (1) The vertical structure of the disk in ordinary spiral galaxies is well described as a locally self-gravitating, isothermal sheet. (2) The scale height of the disk is independent of distance from the nucleus within each galaxy. (3) These results hold for galaxies with both small (e.g., NGC 4244, NGC 5907) and large (e.g., NGC 891, NGC 7814) bulge-to-disk ratios.

What is the disk structure of barred galaxies? According to Kormendy (1979, 1981), distinct components of barred galaxies include spheroids, bars, lenses, and, in some cases, outer (pseudo) rings. He suggested that outer rings are a result of H I gas falling into a ring-shaped minimum in the bar potential, and that lenses originate from a bar through a still unknown interaction of the bar with a spheroidal bulge, which makes some bars evolve away to a nearly axisymmetric state. Recently, kinematical properties of barred galaxies have been studied extensively by Kormendy (1981, 1982*a*, 1983). To attack the problems of barred spiral galaxies further, it is very important to obtain information about the vertical structure of bars, lenses, and outer rings.

For this purpose, we have obtained surface photometry of NGC 4762, which is classified as SB(r)0? in the *Second Reference Catalogue of Bright Galaxies* (de Vaucouleurs, de Vaucouleurs, and Corwin 1976; hereafter RC2). Indeed, NGC 4762 is believed to be an early-type *barred* galaxy (see § III) and to be seen perfectly edge-on (Burstein 1979*c*). It is a member of the Virgo cluster of galaxies (de Vaucouleurs 1961). For its distance we adopt 14.5 Mpc (Hanes 1982), so $1'' = 70$ pc. Details for the data analysis, reduced data, and comparison with previous studies are presented in a separate paper (Hamabe and Wakamatsu 1984).

II. OBSERVATIONS AND REDUCTION

In order to examine the detailed structure of the bright inner region, two short-exposure plates were obtained, in good seeing, with the 2.5 m duPont telescope at the Las Campanas Observatory. For the faint outer region, two long-exposure plates were taken with the Palomar 1.2 m Schmidt telescope and the 1.05 m Kiso Schmidt telescope at the Tokyo Astronomical Observatory. Prints from these plates are shown in Figures 1*a* and 1*b* (Plates 6 and 7), and a journal of the plates is listed in Table 1.

The reduction procedures were similar to those described in previous papers (Hamabe *et al.* 1979, 1980; Hamabe and Okamura 1982; Hamabe 1982). They are briefly described here. The plates were digitized using a PDS microdensitometer. For the Las Campanas plates, a square aperture of size 50 μm (0.″54) was used. An area of $18.'4 \times 9.'2$ centered on the galaxy was digitized, resulting in matrices of size 2048×1024.

[1]Guest Investigator at the Hale Observatories.

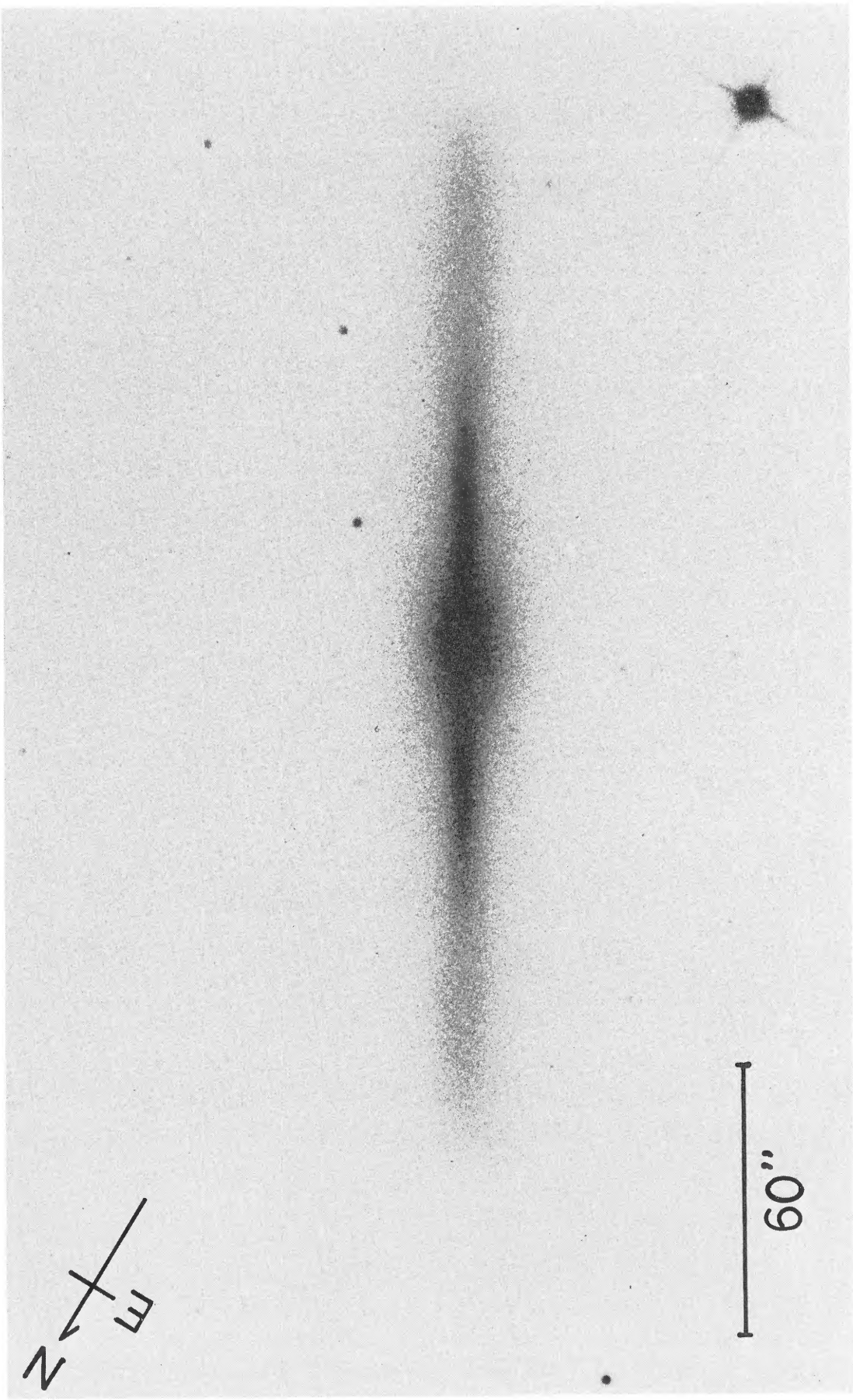

FIG. 1*a*.—A short exposure, duPont telescope plate (CD 1010) of the edge-on galaxy NGC 4762. The inner bright part of the disk is extremely thin and is identified as a bar seen obliquely at an angle $\phi = 33° \pm 10°$ to the line of sight.

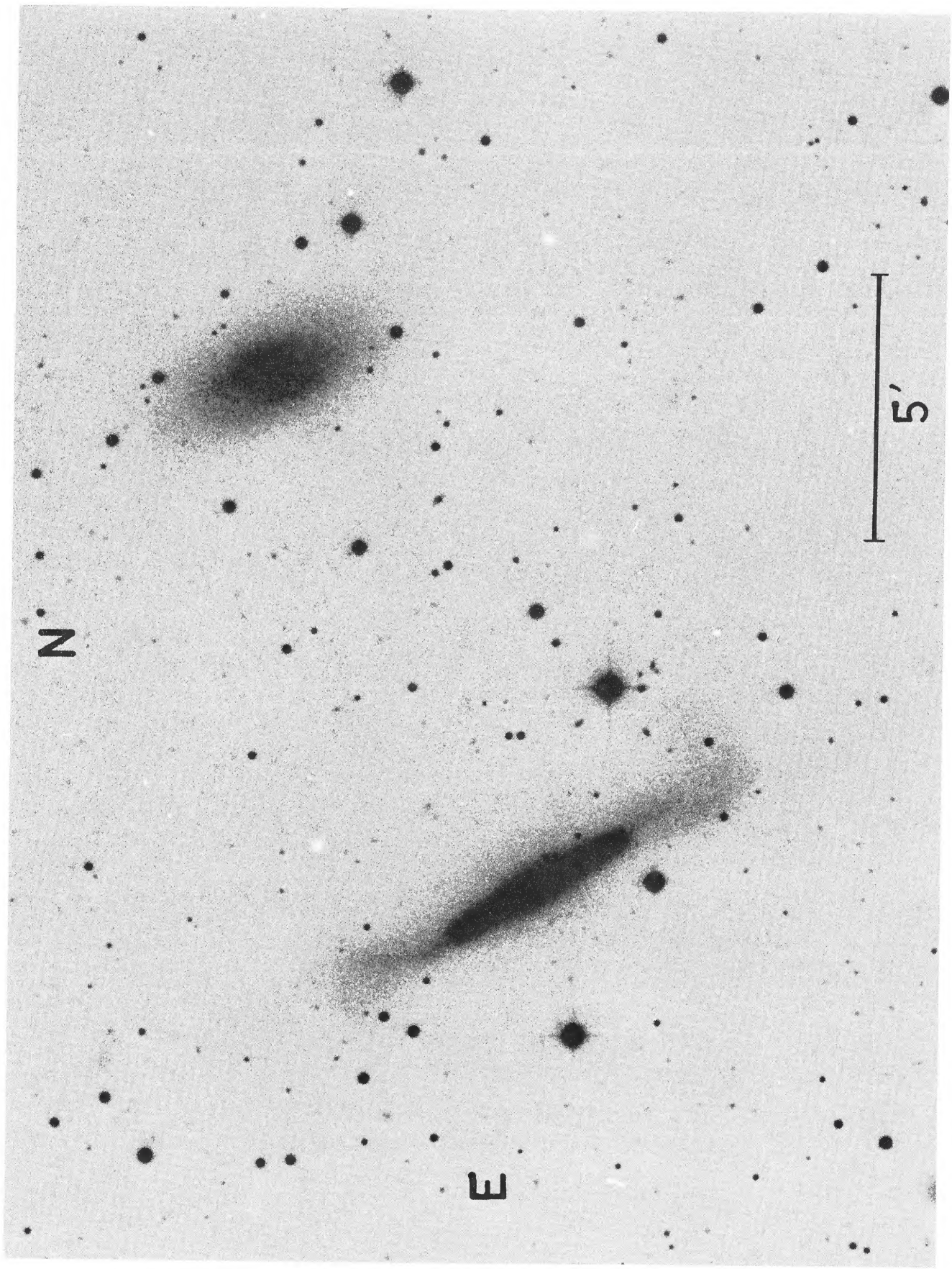

FIG. 1*b*.—A deep IIIa-J, Palomar Schmidt plate of the field NGC 4762. The faint outer envelope of NGC 4762 is identified as an outer warped ring. The bright SB(r)0$^-$: galaxy 10'5 NW of NGC 4762 is NGC 4754.

TABLE 1

LOG OF PLATES OF NGC 4762

Plate Number	Date (1979)	Telescope	Plate Scale (arcsec mm^{-1})	Emulsion	Filter	Exposure (min)
CD 1010.....	May 23	2.5 m duPont	10.8	103a-O	GG 385	15
CD 1011.....	May 23	2.5 m duPont	10.8	103a-O	GG 385	4
PS 26022.....	May 19	Palomar Schmidt	67.1	IIIa-J	Wr 2C	75
K2222	May 23	Kiso Schmidt	62.5	IIa-O	GG 385	30

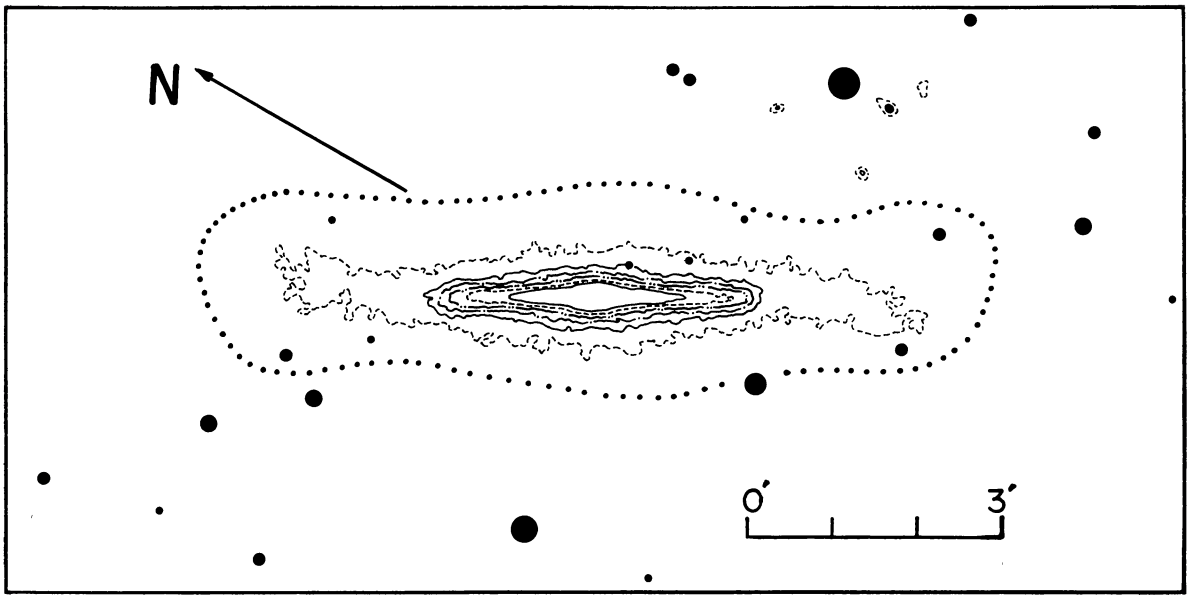

FIG. 2*a*

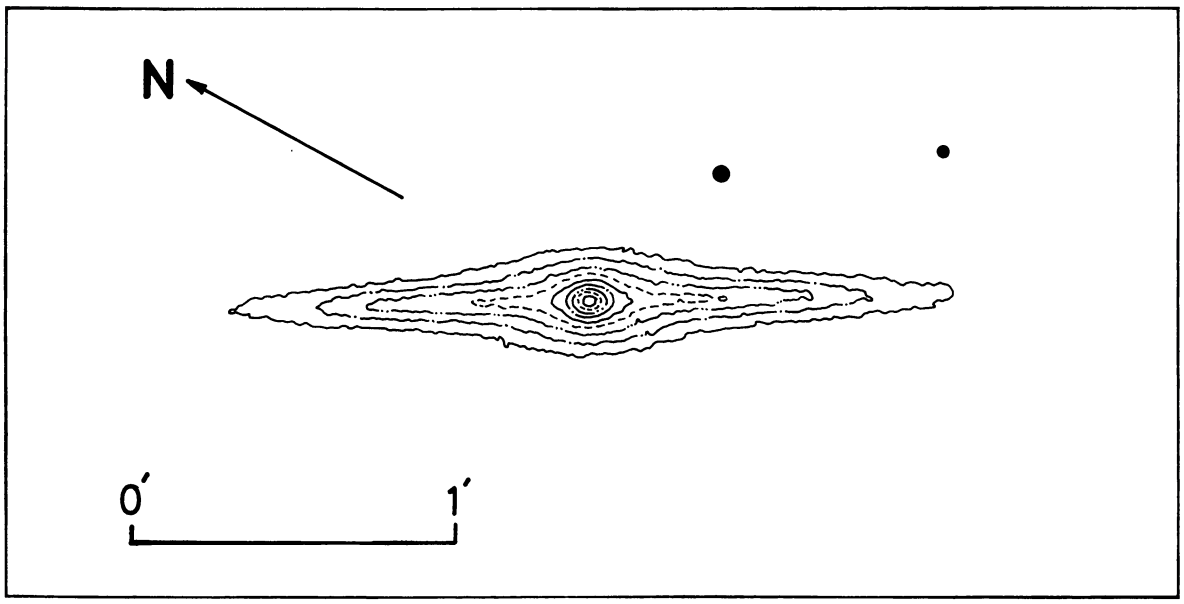

FIG. 2*b*

FIG. 2.—(*a*) Blue isophotes of the nuclear and intermediate region of NGC 4762 from the duPont telescope plates. Isophotes are at 0.50 mag intervals from $\mu_B = 17.0$ to 21.0 mag $arcsec^{-2}$. Axes x and z are along the major and minor axes of the galaxy, respectively. (*b*) Blue isophotes of the outer regions of NGC 4762 from the Kiso Schmidt plate. Isophotes are at 0.5 mag intervals from $\mu_B = 21.0$ mag $arcsec^{-2}$ (*inner solid line*) to $\mu_B = 24.0$ mag $arcsec^{-2}$ (*outer broken line*). The outermost isophote (*dotted line*) is at $\mu_B = 25.5$ mag $arcsec^{-2}$. A slightly asymmetric structure can be seen at the faintest two levels, suggesting the warping of the outer ring.

For the Kiso Schmidt plate, a square aperture of size 20 μm (1".25) was used. An area of 21'.3 × 10'.7 was measured, resulting in a matrix of a size 1024 × 512. The photographic densities were transformed into intensities using step wedges. By averaging 16 × 16 submatrices of the raw galaxy data, we obtained matrices of a size 128 × 64 (Las Campanas plates) or 64 × 32 (Kiso plate). These were used to determine the sky level. This was done by fitting a fifth- or third-order polynomial to each sky matrix. The data were then sky-subtracted. The final analysis is based on the sum of two Las Campanas plates and one Kiso plate. The zero point of the luminosity scale was determined from published photoelectric multiaperture photometry (see Tsikoudi 1977). In Figures 2*a* and 2*b*, isophotal maps are shown. We define a coordinate system centered on the galaxy whose x- and z-axes are the major and minor axes, respectively. We refer to profiles parallel to the major and minor axes as x- and z-profiles, respectively.

As seen in Figures 1*a* and 1*b*, NGC 4762 is almost symmetric with respect to both the major and minor axes, except for the outermost parts ($x > 3'$). Therefore, we folded the data around the major and minor axes, and averaged the four quadrants. Two series of x- and z-profiles are shown in Figures 3 and 4. Comparisons with previous studies (van Houten 1961; Burstein 1979*a*, *c*; Tsikoudi 1980) are, in general, in good agreement (Fig. 5) and are described in detail in Hamabe and Wakamatsu (1984).

III. EVIDENCE FOR AN EDGE-ON BARRED GALAXY

a) Identification of Components

In this section, we suggest that NGC 4762 is an edge-on barred galaxy with its bar oriented obliquely to the line of sight. Because it is edge-on, however, we cannot unambiguously recognize the bar. Instead, we are forced to use circumstantial evidence. As pointed out by Kormendy (1979, 1981, 1982*b*), early-type barred galaxies are characterized by spheroids, bars, lenses, and in some cases, outer rings. Here we suggest which part of NGC 4762 correspond to the above four components.

The major-axis profile of NGC 4762 has a very peculiar shape (Figure 3). It shows four distinct components. The bulge is the very bright component which dominates at $x \leq 15''$. The second feature is a hump at $20'' \leq x \leq 60''$: The third has a shallow luminosity gradient in the region $60'' \leq x \leq 105''$ and with a sharp outer edge at $x \approx 110''$. The fourth component is very extended and lies beyond $x = 115''$. This complicated profile means that NGC 4762 has a more sophisticated structure than ordinary spiral galaxies, which are composed mainly of a spheroidal bulge and a truncated exponential disk (van der Kruit and Searle 1981*a*, *b*, 1982*a*, *b*; Jensen and Thuan 1982). This peculiar feature, originally detected by Burstein (1979*a*) and Tsikoudi (1980), made NGC 4762 to be classified as SB(r)0? in RC2 (de Vaucouleurs 1982).

We focus our attention upon the behavior of the second and the third components in a series of x-profiles (Fig. 3). The second component is most clearly distinguished from the third one in the major axis profile ($z = 0''$). It becomes more and more insignificant at larger z distance and finally disappears completely in the profile at $z = 6''$. In the profiles above $z = 6''$, the third component replaces it and becomes the major contributor in the region $20'' \leq x \leq 105''$. These features imply that there are two distinct components with different scale heights in the z-direction. We identify the flatter component (lying $20'' \leq x \leq 60''$) as the bar and the thicker one (lying $20'' \leq x \leq 105''$) as the lens. As illustrated in Figure 6, if an edge-on bar of a length a is observed obliquely, i.e., $0° < \phi < 90°$, where ϕ is the angle between the major axis of the bar

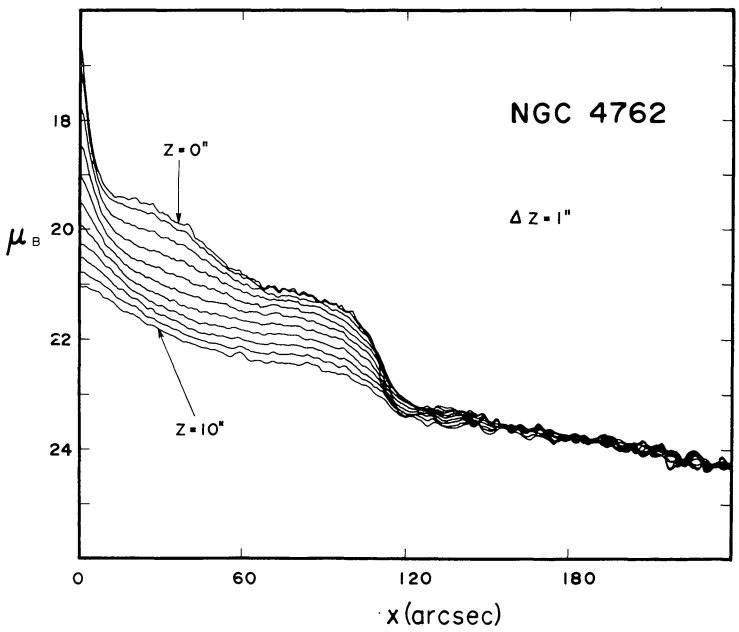

FIG. 3.—The x profiles, i.e., observed luminosity profiles parallel to the major axis. The scans were made at 1" intervals from $z = 0''$, the major axis, to $z = 10''$. The second component, appeared as a hump lying in $20'' \leq x \leq 60''$, is prominent at $z = 0''$ and becomes insignificant at $z \geq 6''$.

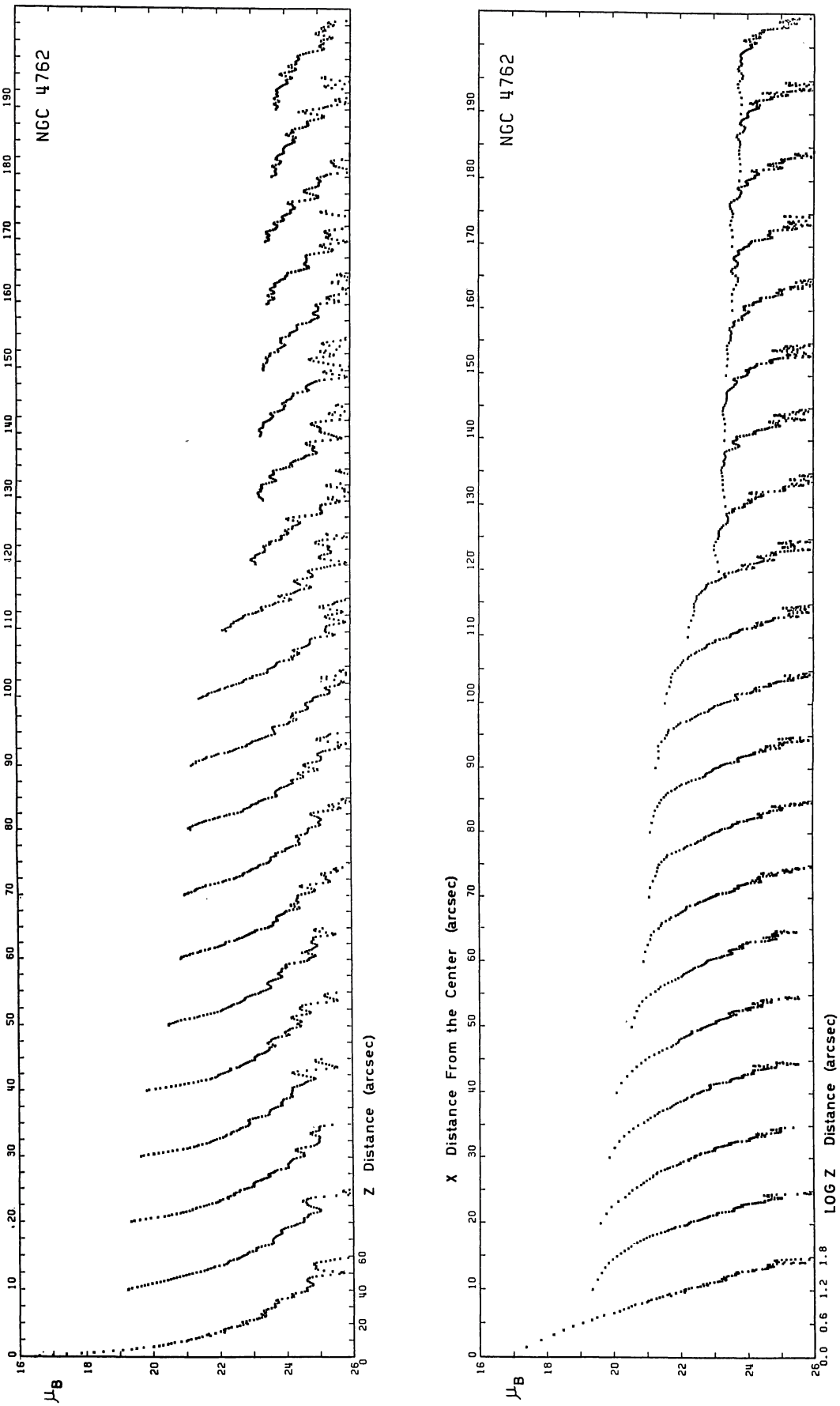

FIG. 4.—The z profiles, i.e., observed profiles perpendicular to the major axis. The scans were made at 10″ intervals from $x = 0''$, the minor axis, to $x = 190''$. The abscissa z is plotted in the linear scale (a) or in the logarithmic scale (b). The profiles change significantly from the inner to the outer regions.

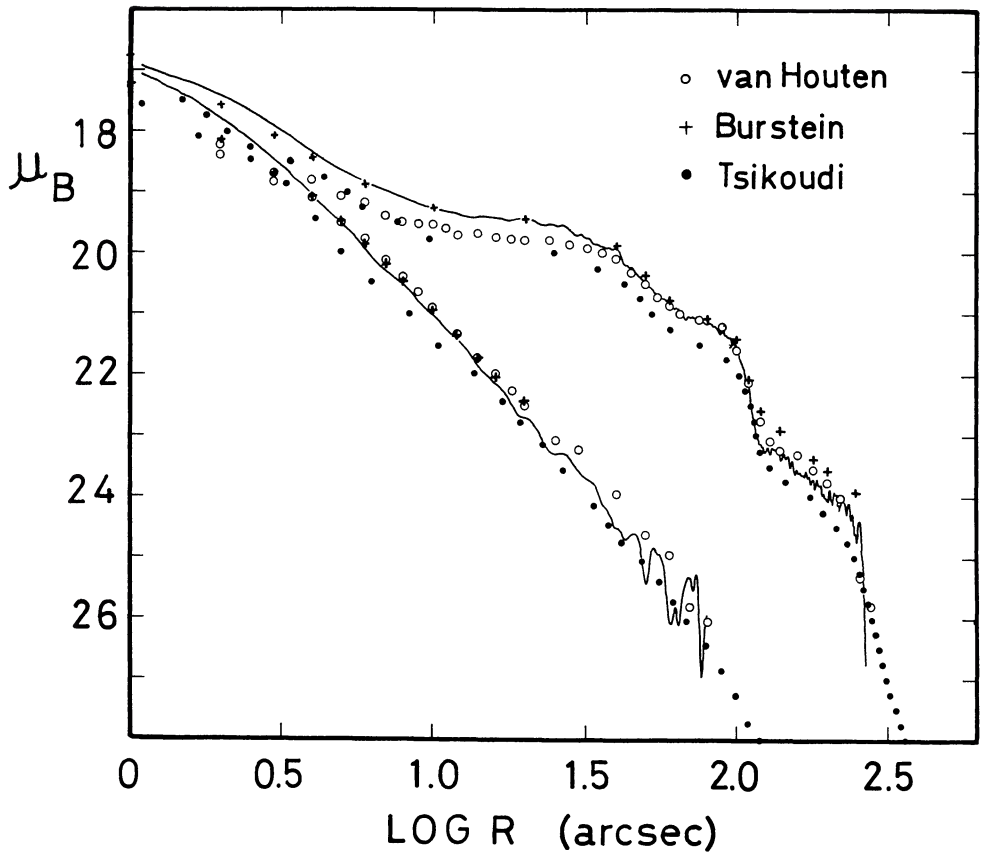

FIG. 5.—Major or minor axis profiles of the present data (*solid lines*) are compared with the previous studies by van Houten (1960), Burstein (1979*a*), and Tsikoudi (1980).

and the line of sight, then at $0° < x < (a/2) \sin \phi$, the bar and the lens are seen superposed on each other. At larger radii, $(a/2) \sin \phi < x < a/2$, only the lens is seen. This configuration can explain the abrupt change of the profiles, seen at $x \approx 60''$ in Figure 3.

b) Evidence for a Barred Galaxy

First of all, we present evidence that the fourth component is probably an outer pseudo ring.[2] By assuming axial symmetry of the galaxy, we can estimate how the profile would appear if the galaxy were face-on. The method of calculation was described in Watanabe, Kodaira, and Okamura (1982), and the rectified profile is shown in Figure 7. We find a shallow dip ($120'' < r < 180''$) and a broad prominent hump ($180'' < r < 270''$). Similar features can be seen in the independent analysis in V color band by Watanabe, Kodaira, and Okamura (1982). So these may be real features, although somewhat marginal because of their faintness. This fact suggests that there is a pseudo-ring which is nearly detached from the main body of the galaxy. The pseudo-ring may be wide in width, and have a very shallow luminosity gradient. The features are consistent with the appearance of face-on outer rings in SB0 and SBa galaxies (Sandage 1961, hereafter The Hubble Atlas; Kormendy 1979). In this case, the outer pseudo-ring happens to be slightly warped (Fig. 1b), as seen in some SB0 galaxies (Kormendy 1979).

Next we examine whether the bar and the lens identified in § III*a* have common properties as those in typical SB0 galaxies have. According to Kormendy (1979), the surface brightness of a bar along its long axis is nearly constant interior to a sharp outer edge. A lens also has a very shallow brightness gradient inside a sharp outer edge. Such *sharp outer edges both of the bar and lens of NGC 4762* are shown in the major axis profile (Fig. 3) and the rectified face-on profile (Fig. 7) at $x \approx 60''$ and $105''$, respectively. *The shallow luminosity gradient of the lens* is clearly seen as a plateau ($65'' \lesssim r \lesssim 105''$) in Figure 7. *The shallow brightness gradient of the bar* is diluted by projection and will be discussed in § V*c*. The contrast of surface brightness between the bar and the lens, if seen face-on, is ~ 0.72 (§ V*c*) and seems reasonable for a galaxy classified as early-type barred. The bar contains about a fraction 0.1 of the total light of the galaxy (§ V*c*).

[2]NGC 4762 is located in a fairly sparse region near the eastern edge of the Virgo cluster, so the only identifiable candidate for a perturbing galaxy is NGC 4754, an SB(r)0$^-$: galaxy 10.5 away. As pointed out by Tsikoudi (1980), the velocity difference of the two galaxies ($\Delta V = 500$ km s^{-1}; Sandage and Tammann 1981) is too large to cause a strong tidal interaction. On our deep IIIa-J Schmidt plate (Fig. 1b), NGC 4754 has no tidal debris (e.g., plumes, wisps, and bridges) nor distortion suggesting that it might be a perturbing galaxy. So, we cannot identify any counterparts involving presumable tidal interactions.

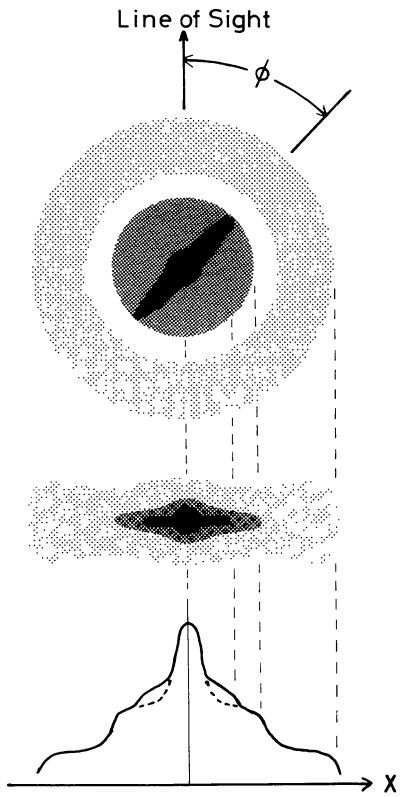

FIG. 6.—Illustration for projection of an early-type barred galaxy. Upper or middle panels are for face-one or edge-on view, respectively. Bottom panel is a schematic luminosity profile along the major axis for the edge-on view. Orientation of the bar is defined as an angle to the line of sight.

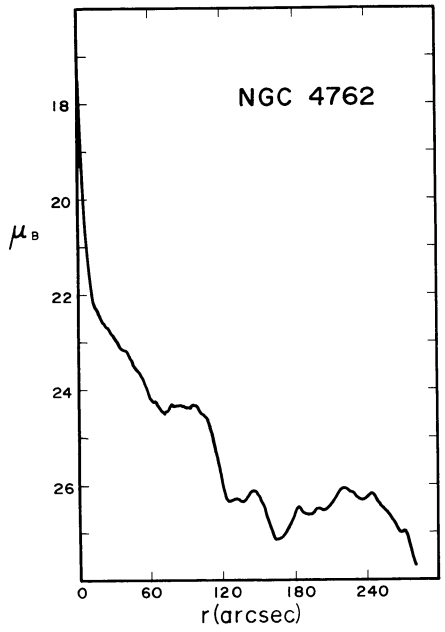

FIG. 7.—Blue, rectified face-on luminosity profile of NGC 4762. Circular symmetry is assumed. Four distinct components are recognized: a nucleus and a nuclear bulge ($0'' \leq r \leq 15''$), a bar superposed on a lens ($15'' \leq r \leq 65''$), a fairly uniform lens ($65'' \leq r \leq 105''$), and a detached outer pseudo-ring ($150'' \leq r \leq 260''$).

Further evidence for the proposed morphology is provided by the diameters of the features observed. Kormendy (1979) found that *the sizes of lenses and outer rings are well correlated with the absolute magnitudes of parent galaxies*. We take $D_L = 210'' \pm 10'' = 14.7 \pm 0.7$ kpc as the lens diameter and $M_B = -20.2$ as the absolute magnitude calculated from a corrected magnitude $B_T = 10.61$ in RC2. Referring to Figures 3 and 5 of Kormendy (1979), we conclude that the linear diameter of the lens of NGC 4762 is typical for the (rather high) luminosity of the galaxy. A similar conclusion can be obtained for the linear diameter of the outer ring; we adopt $D_R = 500'' \pm 20'' = 35.1 \pm 1.4$ kpc. (The above examinations are made on Kormendy's distance scale 22.5 Mpc to the Virgo cluster.) In addition, *the ratio of the ring diameter to the bar diameter* is 2.4 ± 0.2. This is consistent with the average value 2.21 ± 0.12 for 13 barred galaxies found by Kormendy (1979) and Athanassoula *et al.* (1982). This ratio is of interest, because it has been interpreted as a consequence of resonance effects produced by the bar (Athanassoula *et al.* 1982).

A problem for our identification of this galaxy as an early-type barred galaxy is that the size of the nuclear bulge might be too small to be classified so. On the photographs in The Hubble Atlas, nuclear bulges of early-type barred galaxies always stick out from their bars. The diameter of the nuclear bulge of NGC 4762, estimated from Figures 3 and 7, is $\sim 40''$, which is comparable to the width of the bar estimated on the assumption of $(b/a)_{\rm bar} = 0.19 \pm 0.03$. Besides, the bulge-to-disk ratio $\gamma = 0.3$ (§ IV) suggests that the bulge is fairly small (see Yoshizawa and Wakamatsu 1975; Burstein 1979*b*; Boroson 1981). So NGC 4762 may have a small bulge for an early-type barred galaxy, although we can find other early-type barred galaxies with small bulges, such as NGC 2217.

We should examine whether the second thin component could be identified with either *an inner ring* or *a spiral arm* of an ordinary (i.e., nonbarred) galaxy. Most of the inner rings of ordinary spiral galaxies are very prominent when seen face-on (The Hubble Atlas; de Vaucouleurs and Buta 1980; Buta and de Vaucouleurs 1982). So the second component of NGC 4762 would appear as a sharp hump on a rectified face-one profile, if it were surely an inner ring. Figure 7 shows, however, no evidence for the presence of a ring structure in the region $20'' \leq r \leq 60''$. If the second component of NGC 4762 could be identified with a spiral pattern, an abrupt change of the luminosity profile on the main disk at $r \approx 60''$ (Figs. 3 and 7) could be attributed to the presence of dual (inner and outer) spiral arms like in NGC 1068 and NGC 4736 (see The Hubble Atlas). These galaxies with dual spiral arms have sometimes outer (pseudo) rings (The Hubble Atlas; Hodge 1968). However, they may be limited to morphological types later than Sab and not be found among such early-type galaxies as NGC 4762. Throughout the body of NGC 4762, there are no dust lanes, H II regions, nor star clusters suggesting it to be classified as a spiral galaxy. Here we note that the second component is not blue when compared with surrounding regions (Hamabe *et al.* 1981).

Another argument against an ordinary spiral galaxy hypothesis is that *early-type galaxies with outer rings are limited mainly to barred galaxies*. According to *A Revised Shapley-Ames Catalogue of Bright Galaxies* (Sandage and Tammann

1981), only two *ordinary spiral* galaxies (NGC 254[3] and NGC 7020) have outer rings among 138 S0 or S0/Sa galaxies, while 10 *barred* galaxies do have outer rings among 47 SB0 or SB0/SBa galaxies. Therefore, it may be implausible that the second component is just a spiral pattern of a normal spiral galaxy, although it can not be completely disproved.

Finally, we estimate the orientation angle ϕ (see Fig. 6). If a uniform bar of a length a and width b is seen obliquely at an angle ϕ, then the projected length of the bar D_B is expressed as

$$D_B = a \sin\phi + b \cos\phi. \quad (1)$$

If the lens is assumed as circular when seen face-on [their mean axial ratio in other SB galaxies is $(b/a)_{\rm lens} = 0.85$: see Kormendy 1979 and Athanassoula *et al.* 1982], then its projected diameter D_L is nearly equal to a. Thus, we obtain a relation

$$D_B/D_L = \sin\phi + (b/a)_{\rm bar} \cos\phi. \quad (2)$$

Taking $D_B = 130'' \pm 10''$, $D_L = 210'' \pm 10''$, and $(b/a)_{\rm bar} = 0.19 \pm 0.03$, a mean value roughly estimated from 12 galaxies in The Hubble Atlas and in Kormendy (1979), we get $\phi = 27^\circ{}^{+3^\circ}_{-6^\circ}$. This is a lower limit, because a luminosity profile of a bar along its minor axis is generally not flat but steep as in a one-fourth law (Kormendy 1982*b*). If $b = 0$, ϕ could be as large as $\phi = 38^\circ{}^{+6^\circ}_{-5^\circ}$. We adopt $\phi = 33^\circ \pm 10^\circ$, the mean of the above two estimates.

IV. NUCLEAR BULGE AND OUTER RING

We first examine the structure of the bulge and the ring, and then estimate their light contributions that should be subtracted from the observed profiles when we study the vertical structure of the bar and the lens in the next section.

From the isophotal maps (Fig. 2*a*; see also Fig. 11 of Tsikoudi 1980), the innermost contours are elliptical with axial ratio $(b/a)_{\rm bulge} = 0.8$. There is no trace of a cusp due to the disk component, indicating that the bulge is dominant at this level. On the contrary, several contours fainter than $\mu_B = 20.0$ mag arcsec^{-2} are of similar shape, implying that the bulge has a negligible contribution. The nuclear bulge is approximated by a de Vaucouleurs's one-fourth law with an effective radius of $z_e = 4'' \pm 0''.5$, effective brightness $\mu_e = 19.2 \pm 0.1$ mag arcsec^{-2}, and axial ratio $(b/a)_{\rm bulge} = 0.7$. These parameters were determined in such a way that the spherical component should disappear nearly completely on the decomposed isophotes that were made by subtracting the bulge component from the observed isophotes. Here we cannot determine the axial ratio of the bulge unambiguously, because the nuclear bulge is too small to yield a precise value, and because bulges in general change their ellipticities along their radii (Boroson 1981; Monet, Richstone, and Schechter 1981). We take the conservative value $(b/a)_{\rm bulge} = 0.7$. This makes the estimated bulge contribution to the bar and lens profiles as large as possible. Details for the decomposition are described in Hamabe and Wakamatsu (1984). These parameters yield the luminosity of the bulge $L_{\rm bulge} = 2.5 \pm 0.5 \times 10^9\ L_\odot$ and the bulge-to-disk ratio $\gamma = 0.3$. Uncertainties of the parameters of the bulge do not seriously affect the intrinsic profiles of the lens and bar components studied in § V, because the bulge contributes very little to the z-profiles beyond $x \approx 25''$ (Figs. 8*a*–8*c*).

The z-profiles beyond $x = 115''$ are clearly broader than those inside $x = 105''$ (Fig. 4). This indicates that the outer ring is more extended than the lens and bar. The vertical profiles of the ring are essentially in similar shape at each x-position but get slightly broad toward the edges. It could be due to a deviation from circular symmetry and also due to the warp. The z-profile at $x = 140''$ is fitted to Camm's (1950) case II model (§ V*a*) with either $n = \infty$ and $\bar{z} = 24'' \pm 2'' = 1680 \pm 150$ pc or $n = 1.0$ and $\bar{z} = 28'' \pm 2'' = 1960 \pm 150$ pc. The observed magnitude range of the profile, however, is too small to determine the alternatives. Other parameters characterizing the ring are summarized in Table 2.

Now we estimate the light contribution from the outer ring to the observed z-profiles. Since the ring has a very shallow luminosity gradient in x (Fig. 3), we estimate its contribution at $x \leq 105''$ as observed z-profile at $x = 140''$.

In Figures 8*a*–8*c*, the light contributions to each z-profile of the bulge and ring are shown as dot-dashed and thin lines, respectively. Subtracting these two components from the observed z-profiles, we obtain profiles of the lens and bar at each x-position. These are shown as dotted lines in Figures 8*a*–8*c* and are analyzed in the next section.

V. STRUCTURE OF THE BAR AND LENS

a) Self-gravitating Stellar Disk

We study the kinematical properties of the bar and the lens by comparing their luminosity profiles with the mass models on the assumption of a constant mass-to-luminosity ratio. Camm (1950) has studied the properties of locally self-gravitating stellar disks which are plane-parallel and infinite in radius. His case II model has a vertical velocity dispersion $\sigma(z)$ that increases (becomes hotter) with distance z above the plane. It has infinite extent in z. The structure of the disk is expressed, through a parameter θ, as

$$\rho(z) = \rho_0 (\cos\theta)^{2+2n^{-1}}, \quad (3)$$

and

$$z = \bar{z} \int_0^\theta (\sec\theta)^{1+2n^{-1}}\, d\theta. \quad (4)$$

In the above, $\rho(z)$ and ρ_0 are the mass densities at height z and $z = 0$, respectively, and $\bar{z}$ is the scale height of the disk as defined by

$$\bar{z} = \sigma(0)/(2\pi G \rho_0)^{1/2}. \quad (5)$$

[3]Classified as SAB(r)0?, a transition type, in RC2. The third galaxy NGC 474 = Arp 227 [PSA(s)0; RC2] is a typical example of peculiar galaxies with concentric ripples (Malin and Carter 1980; Carter, Allen, and Malin 1982; Schweizer 1983) and so is rejected.

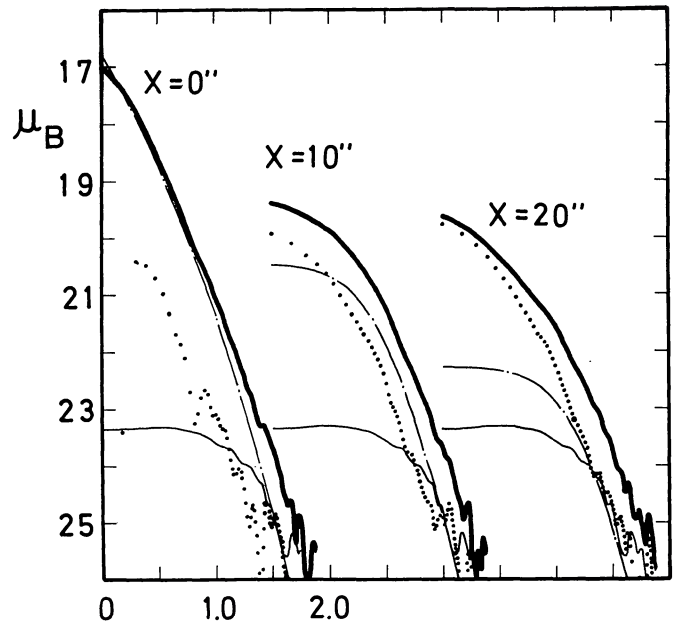

FIG. 8*a*

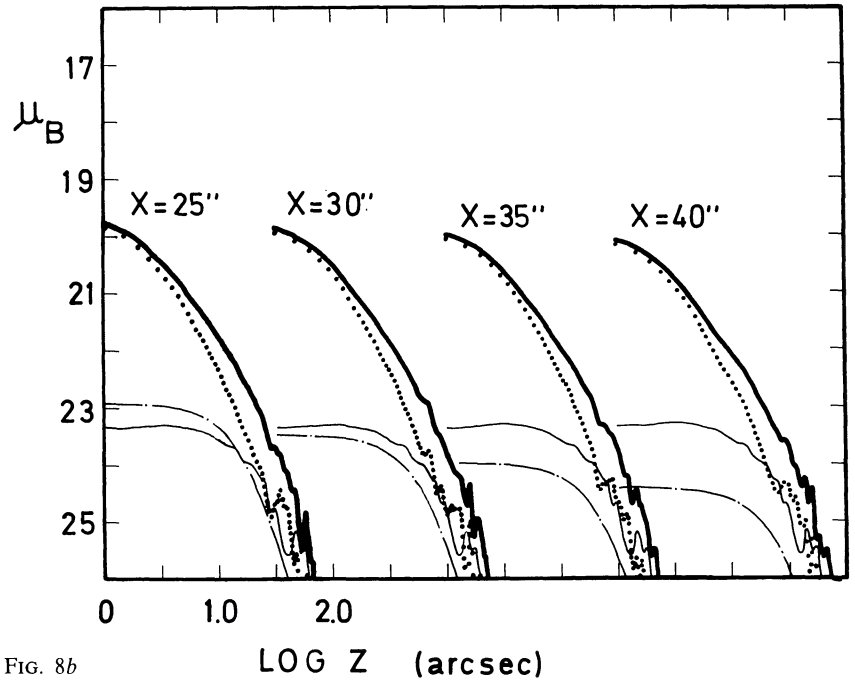

FIG. 8*b*

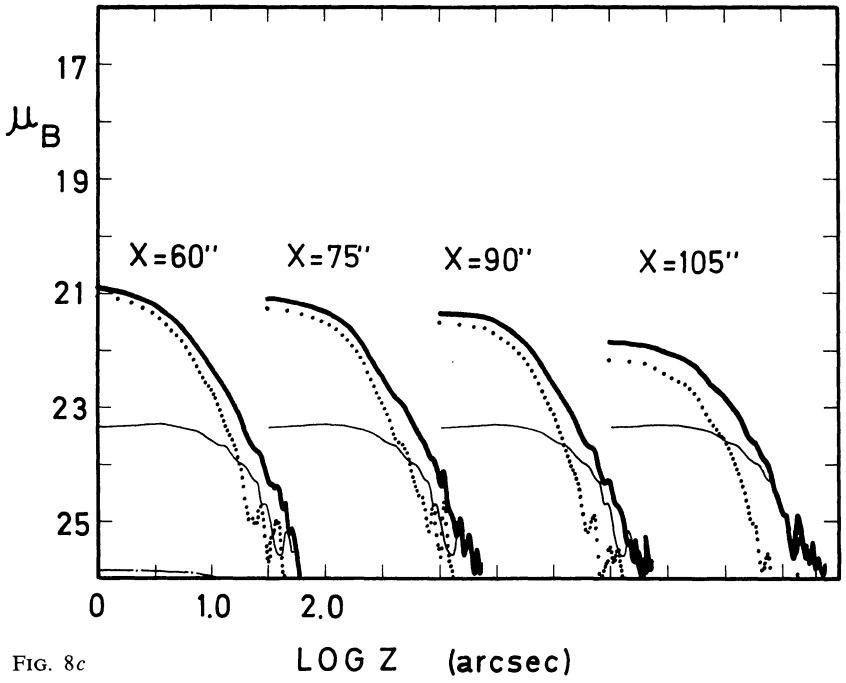

FIG. 8*c*

FIG. 8.—Decomposition fits to the z profiles. The bulge and ring components are plotted in dot-dashed or thin lines, respectively. Dotted lines represent the (observed − bulge − ring) distributions. (*a*) The nuclear region; (*b*) the bar plus lens region; (*c*) the lens region.

TABLE 2

STRUCTURE OF FOUR COMPONENTS OF NGC 4762[a]

Component	Bulge	Bar	Lens	Ring
Measured at	$x = 0''$	$x = 25''$	$x = 60''$	$x = 140''$
Fitting model	1/4 law	Camm's model	Camm's model	Camm's model
Parameter n	...	∞	1.0	∞
Vertical scale height $\bar{z}$				
(arcsec)	4.0 ± 0.5[b]	2.2 ± 0.2	8.0 ± 0.5	24 ± 2
(pc)	280 ± 70[b]	155 ± 15	560 ± 40	1680 ± 150
Surface brightness $\mu_B(0)$ (mag arcsec^{-2})	19.2 ± 0.1[c]	20.5 ± 0.2	21.1 ± 0.1	23.3 ± 0.1
Face-on brightness[d] Σ (mag arcsec^{-2})	20.2 ± 0.2	23.5 ± 0.3	24.2 ± 0.2	26.3 ± 0.2
Luminosity				
($\times 10^8 L_\odot$)	2.5	1.2	3.9	3.3
(fraction)	0.23	0.11	0.36	0.30

[a]Estimated on the distance scale of 14.5 Mpc.
[b]Effective radius.
[c]Effective brightness.
[d]Rectified face-on surface brightness. See the text and Fig. 7.

Here G is the gravitational constant. The surface mass density $M = \int_{-\infty}^{\infty} \rho(z)\, dz$ is expressed

$$M = 2\rho_0 \bar{z} = (2\rho_0/\pi G)^{1/2} \sigma(0). \quad (6)$$

The velocity dispersion at height z is calculated from the velocity distribution function (Camm 1950) as

$$\sigma(z) = \sigma(0)(\sec \theta)^{n^{-1}}. \quad (7)$$

A single parameter n specifies the structure of the disk. As n increases, the vertical gradient of $\sigma(z)$ becomes less steep. The extreme case $n = \infty$ corresponds to an isothermal model,

$$\rho(z) = \rho_0 \operatorname{sech}^2 (z/\bar{z}). \quad (8)$$

b) *Structure of the Lens*

In Figure 9, the decomposed profiles are shown for the lens region $60'' \leq x \leq 90''$. The profiles at $x = 75''$ and $90''$ are shifted along the ordinate upwards by 0.18 and 0.41 mag, respectively, to illustrate the similarity of the profile at $x = 60''$. The meaning of this similarity will be discussed later. As shown in Figure 9, the lens profiles are very well fitted to Camm's (1950) model. The adopted parameters are $n = 1.0$ and $\bar{z} = 8''.0 \pm 0''.5 = 560 \pm 40$ pc. For comparison, an isothermal model ($n = \infty$) is plotted as a dotted line. It does not reproduce the z-profiles, even allowing for the fairly large uncertainties at $z > 15''$. Incomplete subtraction of the outer ring component could result in such a deviation from an isothermal model. If the region $z > 15''$ is dominated by the light from the outer ring, the faintest contours on the isophotal map should be concave due to the projected nature of an edge-on ring. As can be seen from Figure 2*b*, however, the contours of the faintest two levels are clearly convex. Besides the convex shape terminates at $x = 105''$, which coincides with the edge of the lens. Therefore, the regions concerned are not dominated by the light of the outer ring, but have the light contributions both from the ring and the lens (see Fig. 8*c*), unless the ring deviates significantly from circular symmetry. So, the extended system beyond $z = 15''$ is certainly associated with the lens and should be seen as the extended part of the lens system. This is the component which led Burstein (1979*c*) to identify it as the *thick disk*.

The lens is found to be a very different structure from the disks of ordinary spiral galaxies, for which van der Kruit and Searle (1981*a*, *b*) showed that projected vertical profiles are well fitted to isothermal models with a constant scale height. Does the deviation from an isothermal model imply the possibility that the lens might be locally isothermal, but with changing scale height along the radius, and so along the line of sight? This is definitely not correct, because, the z-profiles do not change shapes at different x-positions (Fig. 9). So the lens has a constant structure along the radius and deviates intrinsically from an isothermal model.

Such deviations were first observed in disks of some S0 galaxies as thick disks (Burstein 1979*c*) and also detected in some ordinary spiral galaxies (e.g., NGC 891, NGC 4565; van der Kruit and Searle 1981*a*, *b*; Jensen and Thuan 1982) and in our Galaxy (Hill, Hilditch, and Barnes 1979; Gilmore and Reid 1983). According to Burstein (1984), the thick disk found in S0's, as in the present case, has little or no radial gradient in luminosity, while the extended components detected in NGC 891 and NGC 4565 have a strong radial gradient. Van der Kruit and Searle (1981b) suggest that thick disks in spiral galaxies might be attributable to a spheroidal component flattened as a result of the strong gravitational force of the massive disks (see Monet, Richstone, and Schechter 1981). The presence of such a deviation in the lens of NGC 4762, however, is interesting, because it occurs even in a galaxy which has a very small spheroidal component.

We summarize that the lens has (1) a vertical structure which is constant in radius, (2) a scale height independent of radius at least for $60'' \leq r \leq 105''$, and (3) a vertical density gradient which is less steep than that of an isothermal model.

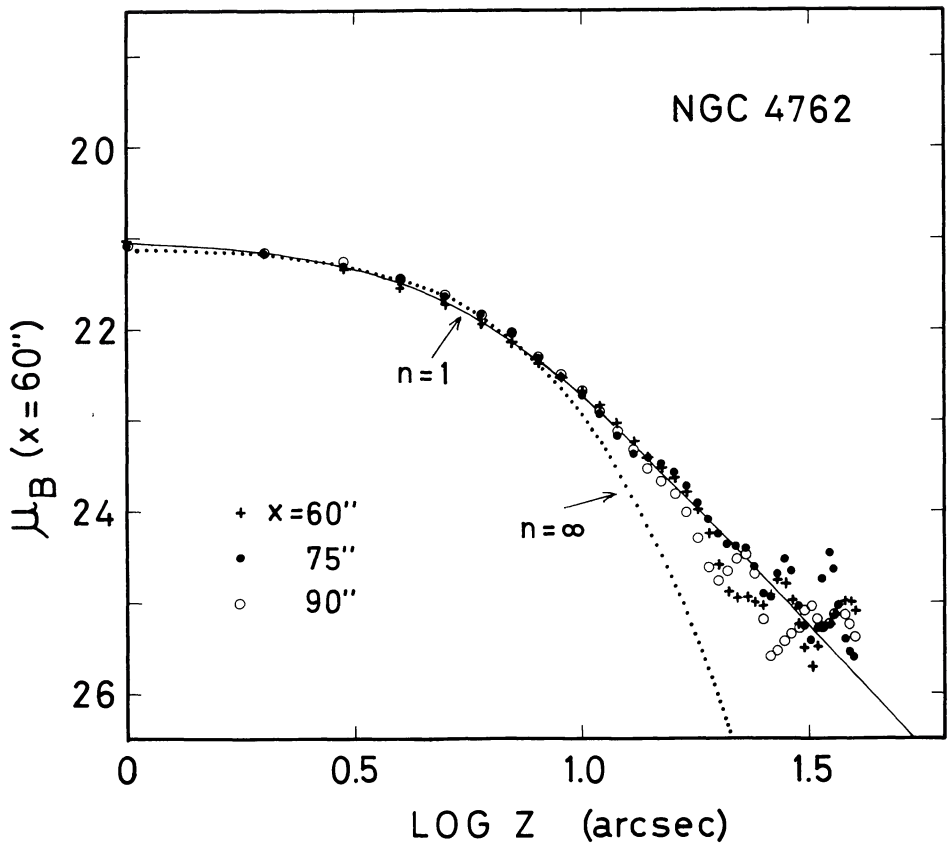

FIG. 9.—Decomposed lens profiles at various distances x from the nucleus. Profiles are shifted along the ordinate to show that the profiles are similar with each other. They are well fitted to Camm's (1950) case II model with parameters $n = 1.0$, $\bar{z} = 8''.0 \pm 0''.5$. A profile of an isothermal model ($n = \infty$) is shown in dotted lines for comparison.

c) *Structure of the Bar*

We examine the bar plus lens profiles in the region $25'' \leq x \leq 60''$, where the lens and the bar are superposed (see Fig. 6). The profiles at each x-position are found to be well fitted to Camm's (1950) model with parameters $n = 0.5$ and $\bar{z} = 5''.5 \pm 0''.5 = 390 \pm 40$ pc, and so they are, as shown in Figure 10, clearly distinguished from the lens profiles obtained in § V*b* (Fig. 9).

Now we decompose the profiles into the bar and the lens components, properly. As described in § III*a*, the humps ($20'' \leq x \leq 60''$) which are identified with the bar are prominent only in the region $z \leq 6''$ (see Fig. 3). So, the luminosities in the region $z > 6''$ may mostly come from the lens component. To confirm this, we compare each z-profile with the mean lens profile given in Figure 9. By shifting the latter profile upward along the ordinate by 0.40, 0.35, 0.28, and 0.21 mag at $x = 25''$, $30''$, $35''$, and $40''$, respectively, we found that the two profiles fit very well with each other for the region $z > 6''$ (see Fig. 10). This implies (1) that the vertical structure of the lens remains to be similar along the entire lens region ($20'' \leq x \leq 105''$) and (2) that the lens has a very shallow luminosity gradient along the radius. The latter is, as pointed out by Kormendy (1979), one of the basic properties of the lens in early-type barred galaxies. Therefore, it is reasonable to estimate the light contribution of the lens component as shown in the full lines of Figure 10.

Finally, by subtracting these lens contributions from the lens plus bar profiles, we obtain the vertical profiles of the bar at each x-position. They are shown in Figure 10 as open circles.[4] They are quite similar with each other and can be fitted to Camm's model with $n = \infty$ (isothermal case). The scale height $\bar{z}$ is constant along the bar, and $\bar{z} = 2''.2 \pm 0''.2 = 155 \pm 15$ pc. The surface brightness $\mu(0)_{\rm bar}$ of the bar component at $z = 0$ is found to be nearly constant at different x-positions. The above results imply that *the bar, if seen face-on, would have a very shallow luminosity gradient along its major axis*. This is one of reasons why we believe that NGC 4762 is a barred galaxy.

The vertical scale height of the bar is found to be only one-third of that of the lens. This is extremely small compared to the thicknesses of disks in ordinary spiral galaxies, which range from 600 to 1000 pc (van der Kruit and Searle 1982*a*). The isothermal disk of equation (8) can be approximated by an exponential law $\rho(z) = 4\rho_0 \exp(z/\beta)$ for $z \gg \bar{z}$, where $\beta = \bar{z}/2$. For the bar of NGC 4762, we obtain $\beta = \bar{z}/2 = 80$

[4] If we subtract the lens profile shown in Fig. 9 without shifting along the ordinate, the resultant vertical profiles of the bar, shown in Hamabe and Wakamatsu (1984), appear like a superposition of a thin and a thick component. Besides the shapes of the profiles, and so the relative strength of the two components, change systematically along x. These are, we think, unreasonable as the bar profiles, since the bars in early-type galaxies are very uniform along their major axes.

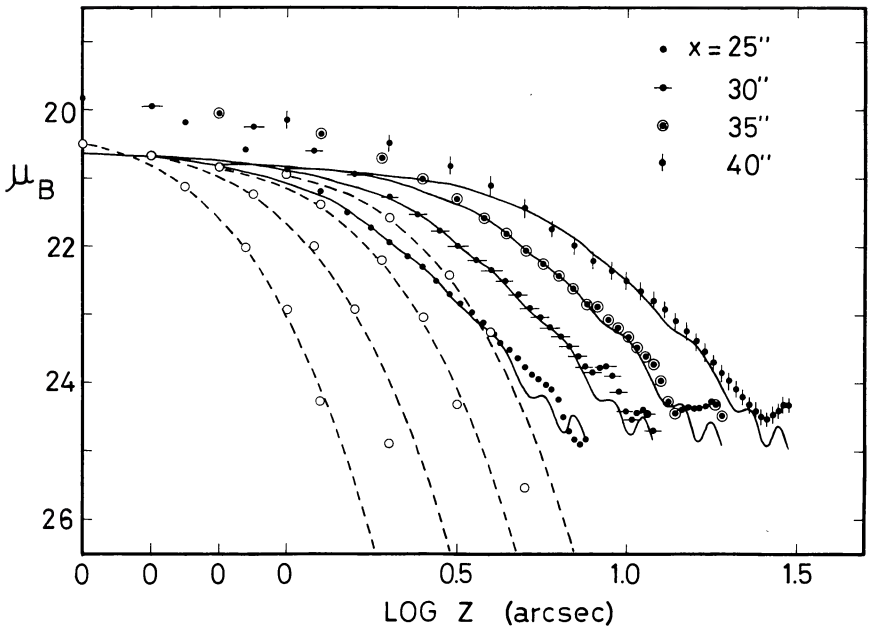

FIG. 10.—Decomposed bar plus lens profiles at different distances x from the nucleus. The light contributions from the superposed lens component are shown in solid lines. The decomposed bar profiles are shown in open circles and fitted to the isothermal model (*broken lines*) with $\bar{z} = 2''.2 \pm 0''.2$.

pc. This is comparable to the thicknesses of the Population I component of our Galaxy. For example, B-type stars have a scale height of 60 pc, and A-type stars have 115 pc (Allen 1973).

We can estimate how prominent the bar would appear, if seen face-on, against the lens, by calculating $\Sigma_{\rm bar}/\Sigma_{\rm lens}$, the ratio of the projected *face-on* surface brightness of the bar to that of the lens. This ratio is

$$\Sigma_{\rm bar}/\Sigma_{\rm lens} = L(0)_{\rm bar}\bar{z}_{\rm bar}/L(0)_{\rm lens}\bar{z}_{\rm lens}, \qquad (9)$$

irrespective of values of the parameter n (see eq. [6]), where $L(0)_{\rm bar}$ and $L(0)_{\rm lens}$ are the volume emissivities of the bar and the lens at $z = 0$, respectively. Both the bar and lens are found to be fairly uniform systems along the radius, and so we obtain the approximate expression,

$$L(0)_{\rm bar}/L(0)_{\rm lens} = [\Lambda(0)_{\rm bar}/\Lambda(0)_{\rm lens}](a/b)_{\rm bar} \sin\phi, \qquad (10)$$

where $\Lambda(0)_{\rm bar}$ and $\Lambda(0)_{\rm lens}$ are the projected edge-on surface luminosities of the bar or lens corresponding to $\mu(0)_{\rm bar}$ and $\mu(0)_{\rm lens}$, respectively. Here we assumed a uniform bar of the length a and the width b as described in § III*b* in order to estimate their projected lengths along the line of sight. Inserting the values $(b/a)_{\rm bar} = 0.19$ and $\phi = 27^{\circ}{}^{+3^{\circ}}_{-6^{\circ}}$ obtained in § III*b* and $\mu(0)_{\rm bar} = 20.5$ and $\mu(0)_{\rm lens} = 20.6$, we obtain $L(0)_{\rm bar}/L(0)_{\rm lens} = 2.6^{+0.3}_{-0.6}$, and so from equation (9), $\Sigma_{\rm bar}/\Sigma_{\rm lens} = 0.72^{+0.07}_{-0.15}$. The contrast of the bar against the lens, if seen face-on, is found to be reasonable as a barred galaxy, although the contrast changes in a large range from galaxy to galaxy (de Vaucouleurs 1975; Okamura 1978).

We conclude the following: (1) The vertical structure of the bar is fairly uniform along its major axis. (2) The surface brightness of the bar, if seen face-on, has a very shallow luminosity gradient along its major axis and has a reasonable contrast to that of the lens. (3) Surprisingly, the vertical scale height of the bar is $\bar{z} = 155 \pm 15$ pc, only one-third of that of the lens. (4) The vertical structure of each component is summarized in Table 2.

VI. DISCUSSION

As can be seen from equation (5), the vertical scale height depends not only on the velocity dispersion but also on the mass density. Does the bar become so flattened due to the deep gravitational potential owing to its high mass density? Or does the bar have completely different kinematical properties, especially in the z-direction, from those of the lens? This is a very crucial point for understanding the structure and formation mechanisms of the bar.

Any star sweeping through the lens will feel, while it is in the bar, a restoring force to the plane which is larger than when it is in the lens. If it has time to respond while still in the bar, its vertical excursion and hence $\bar{z}$ should be reduced. To check this we calculate $P_{\rm osci}$, the vertical oscillation period of the lens, and $P_{\rm cross}$, the plausible time that a star crosses the bar. The former is approximated to be $P_{\rm osci} = 4\ \bar{z}_{\rm lens}/\sigma(0)_{\rm lens} = 5.3 \times 10^7$ yr (the velocity dispersion is estimated below). The latter can be estimated as $P_{\rm cross} = b/(V_{\rm rot} - V_{\rm patt})$, where $V_{\rm rot}$ and $V_{\rm patt}$ are the rotational speed and pattern speed, respectively, and corotation is assumed to occur at or slightly beyond the radius of the bar. We adopt $b = a(b/a)_{\rm bar} = 2 \times 105'' \times 0.19 = 2.8$ kpc, and $V_{\rm rot} - V_{\rm patt} = 110 \pm 20$ km s^{-1} by referring to rotation curves of Bertola and Capaccioli (1978) and Illingworth and McElroy (1981). Then we have $P_{\rm cross} = 2.5^{+0.6}_{-0.3} \times 10^7$ yr. Therefore, stars in the lens may have not enough time to respond the restoring force of the bar. Besides

the mass density contrast of the bar to the lens necessary to reduce the scale height is, from equation (5), $\rho_{\rm bar}/\rho_{\rm lens} = (\bar{z}_{\rm lens}/\bar{z}_{\rm bar})^2 = 13$, if the velocity dispersions of the bar and the lens are similar. The evaluated ratio of the volume emissivities (§ V), however, is $L(0)_{\rm bar}/L(0)_{\rm lens} = 2.6^{+0.3}_{-0.6}$. So the bar may not be so massive to reduce the excursion of the stars in the lens.

We examine the vertical velocity dispersions $\sigma(z)$ of the bar and the lens. We treat the bar as a self-gravitating system, although it is embedded in the potential of the lens. This crude approximation may not be so bad, because the bar has a scale height of only one-third of that of the lens and has a volume emissivity $L(0)_{\rm bar}$ more than twice as large as that of the lens. On the assumption of the constant mass-to-luminosity ratio of the bar and the lens, we have from equation (5)

$$\sigma(0)_{\rm bar}/\sigma(0)_{\rm lens} = \left[\frac{L(0)_{\rm bar}}{L(0)_{\rm lens}}\right]^{1/2} \frac{\bar{z}_{\rm bar}}{\bar{z}_{\rm lens}}. \qquad (11)$$

Inserting the values evaluated in the previous sections, we obtain $\sigma(0)_{\rm bar}/\sigma(0)_{\rm lens} = 0.45^{+0.02}_{-0.05}$. This is significantly less than 1. So the bar must be flattened not due to its strong gravitational potential, but essentially due to its small vertical velocity dispersion.

This conclusion may suggest that the bar is not a system formed from the lens through density enhancement, but is a system having intrinsically different kinematical properties from those of the lens. When it is taken into account that there is no plausible mechanism to cool down a stellar system, the bar might be formed as an intrinsically very cold system like Population I objects in our Galaxy. It is noted that searches for H I emission in NGC 4762 (Bieging 1978; Krumm and Salpeter 1979) yield only an upper limit $M_{\rm H\,I}/L_B = 0.006$ for H I mass to the total luminosity ratio in solar units, which indicates that there is little H I and therefore very few molecular gas clouds that could heat up the stellar systems through scattering.

We estimate the value of $\sigma(0)_{\rm bar}$. We adopt the geometry of the bar as described in § III*b*, and assume a mass to luminosity ratio of 4, based on Bertola and Capaccioli's (1978) mass model of the rotation curve. Then, we obtain, from equation (10), $\rho(0)_{\rm bar} = 5.4^{+0.6}_{-0.8} \times 10^{-1}\ M_\odot\ {\rm pc}^{-3}$, and $\rho(0)_{\rm lens} = 2.1 \pm 0.2 \times 10^{-1}\ M_\odot\ {\rm pc}^{-3}$. These yield $\sigma(0)_{\rm bar} = 19 \pm 2$ km s^{-1}, and $\sigma(0)_{\rm lens} = 42 \pm 2$ km s^{-1}. The errors do not include uncertainty of the uniformity of the bar. The vertical velocity dispersions are much smaller than the velocity dispersion (~ 100 km s^{-1}) in the equatorial plane measured by Illingworth (1981). The bar has an extremely anisotropic velocity dispersion. This is consistent with the results from numerical simulations for bars (e.g., Hohl and Zang 1979; Combes and Sanders 1980).

We wish to thank Drs. J. R. Mould and S. Okamura for loan of their plates and Drs. G. Gilmore, J. Kormendy, and S. Okamura for their critical reading of the draft. We thank also Drs. M. Fujimoto, M. Miyamoto, and B. Takase for discussion and encouragement. One of us (K. W.) is grateful to Drs. T. Boroson, D. Lynden-Bell, J. A. Sellewood, and L. Searle for discussion.

REFERENCES

Allen, C. W. 1973, *Astrophysical Quantities* (London: Athlone).
Athanassoula, E., Bosma, A., Crézé, M., and Schwarz, M. P. 1982, *Astr. Ap.*, **107**, 101.
Bertola, F., and Capaccioli, M. 1978, *Ap. J.*, **219**, 404.
Bieging, J. H. 1978, *Astr. Ap.*, **64**, 23.
Boroson, T. 1981, *Ap. J. Suppl.*, **46**, 177.
Burstein, D. 1979*a*, *Ap. J. Suppl.*, **41**, 435.
_____. 1979*b*, *Ap. J.*, **234**, 435.
_____. 1979*c*, *Ap. J.*, **234**, 829.
_____. 1984, private communication.
Buta, R., and de Vaucouleurs, G. 1982, *Ap. J. Suppl.*, **48**, 219.
Carter, D., Allen, D. A., and Malin, D. F. 1982, *Nature*, **295**, 126.
Camm, G. L. 1950, *M.N.R.A.S.*, **110**, 305.
Combes, F., and Sanders, R. H. 1980, *Astr. Ap.*, **96**, 164.
de Vaucouleurs, G. 1961, *Ap. J. Suppl.*, **6**, 213.
_____. 1975, *Ap. J. Suppl.*, **29**, 193.
_____. 1982, private communication.
de Vaucouleurs, G., and Buta, R. 1980, *Ap. J. Suppl.*, **44**, 451.
de Vaucouleurs, G., de Vaucouleurs, A., and Corwin, H. G., Jr. 1976, *Second Reference Catalogue of Bright Galaxies* (Austin: University of Texas Press).
Gilmore, G., and Reid, N. 1983, *M.N.R.A.S.*, **202**, 1025.
Hamabe, M. 1982, *Pub. Astr. Soc. Japan*, **34**, 423.
Hamabe, M., Kodaira, K., Okamura, S., and Takase, B. 1979, *Pub. Astr. Soc. Japan*, **31**, 431.
_____. 1980, *Pub. Astr. Soc. Japan*, **32**, 197.
Hamabe, M., and Okamura, S. 1982, *Ann. Tokyo Astr. Obs.*, **18**, 191.
Hamabe, M., Okamura, S., Iye, M., and Nishimura, S., 1981, *Pub. Astr. Soc. Japan*, **33**, 643.
Hamabe, M., and Wakamatsu, K. 1984, in preparation.
Hanes, D. 1982, *M.N.R.A.S.*, **201**, 145.
Hill, G., Hilditch, R. W., and Barnes, J. V. 1979, *M.N.R.A.S.*, **186**, 813.
Hodge, P. 1968, *A.J.*, **73**, 846.
Hohl, F., and Zang, T. A. 1979, *A.J.*, **84**, 585.
Illingworth, G. 1981, in *The Structure and Evolution of Normal Galaxies*, ed. S. M. Fall and D. Lynden-Bell (Cambridge: Cambridge University Press), p. 27.
Jensen, E. B., and Thuan, T. X. 1982, *Ap. J. Suppl.*, **50**, 421.
Kormendy, J. 1979, *Ap. J.*, **227**, 714.
_____. 1981, in *The Structure and Evolution of Normal Galaxies*, ed. S. M. Fall and D. Lynden-Bell (Cambridge: Cambridge University Press), p. 85.
_____. 1982*a*, *Ap. J.*, **257**, 75.
_____. 1982*b*, in *Morphology and Dynamics of Galaxies*, ed. L. Martinet and M. Mayor (Sauverny: Geneva Observatory), p. 115.
_____. 1983, *Ap. J.*, **275**, 529.
Krumm, N., and Salpeter, E. E. 1979, *Ap. J.*, **227**, 776.
Malin, D. F., and Carter, D. 1980, *Nature*, **285**, 643.
Monet, D. G., Richstone, D. O., and Schechter, P. L. 1981, *Ap. J.*, **245**, 454.
Okamura, S. 1978, *Pub. Astr. Soc. Japan*, **30**, 91.
Sandage, A. 1961, *The Hubble Atlas of Galaxies* (Washington, DC: Carnegie Institution of Washington).
Sandage, A., and Tammann, G. A. 1981, *A Revised Shapley-Ames Catalogue of Bright Galaxies* (Washington, DC: Carnegie Institution of Washington).
Schweizer, F. 1983, in *IAU Symposium 100, Internal Kinematics and Dynamics of Galaxies*, ed. E. Athanassoula (Dordrecht: Reidel), p. 319.
Tsikoudi, V. 1977, *Pub. Dept. Astr. Univ. Texas-Austin*, No. 10.
_____. 1980, *Ap. J. Suppl.*, **43**, 365.
van Houten, C. J. 1961, *Bull. Astr. Netherlands*, **16**, 1.
van der Kruit, P. C., and Searle, L. 1981*a*, *Astr. Ap.*, **95**, 105.
_____. 1981*b*, *Astr. Ap.*, **95**, 116.
_____. 1982*a*, *Astr. Ap.*, **110**, 61.
_____. 1982*b*, *Astr. Ap.*, **110**, 79.
Watanabe, M., Kodaira, K., and Okamura, S. 1982, *Ap. J. Suppl.*, **50**, 1.
Yoshizawa, M., and Wakamatsu, K. 1975, *Astr. Ap.*, **44**, 363.

MASARU HAMABE: Kiso Observatory, Tokyo Astronomical Observatory, Mitake-mura, Kiso-gun, Nagano-ken 397-01, Japan

KEN-ICHI WAKAMATSU: Physics Department, Junior Technical College, Gifu University, Gifu 501-11, Japan

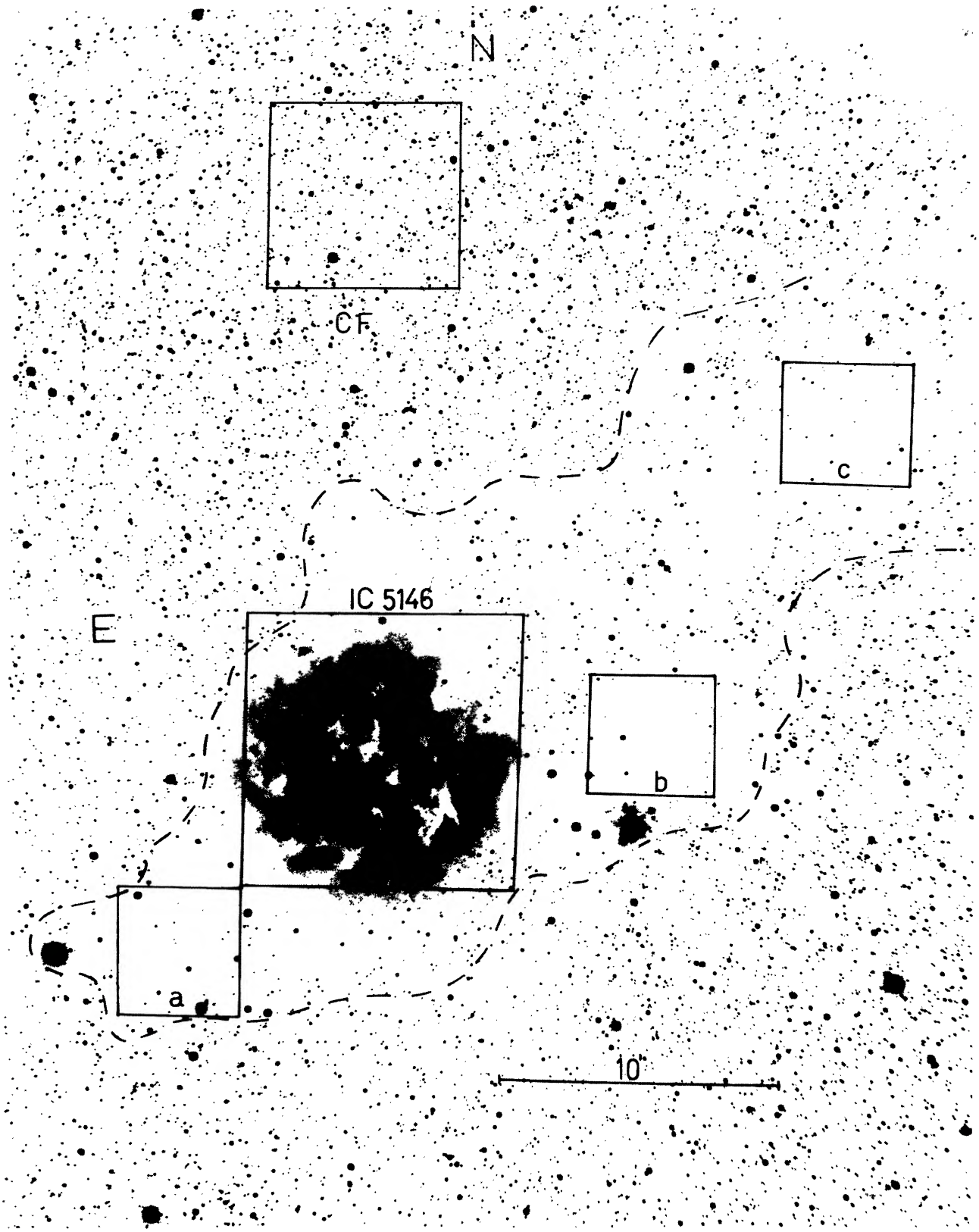

FIG. 1.—Zones under study in this work are identified on an enlargement of the blue plate MPF 3343. They are the "cluster" area (IC 5146); the comparison field (CF), and the three "extinction sampling" areas (a, b, c). Dashed line is the approximate contour of the dark filamentary cloud which extends further to the northwest and out of the shown field.

FORTE AND ORSATTI (*see* page 212)

PLATE 4

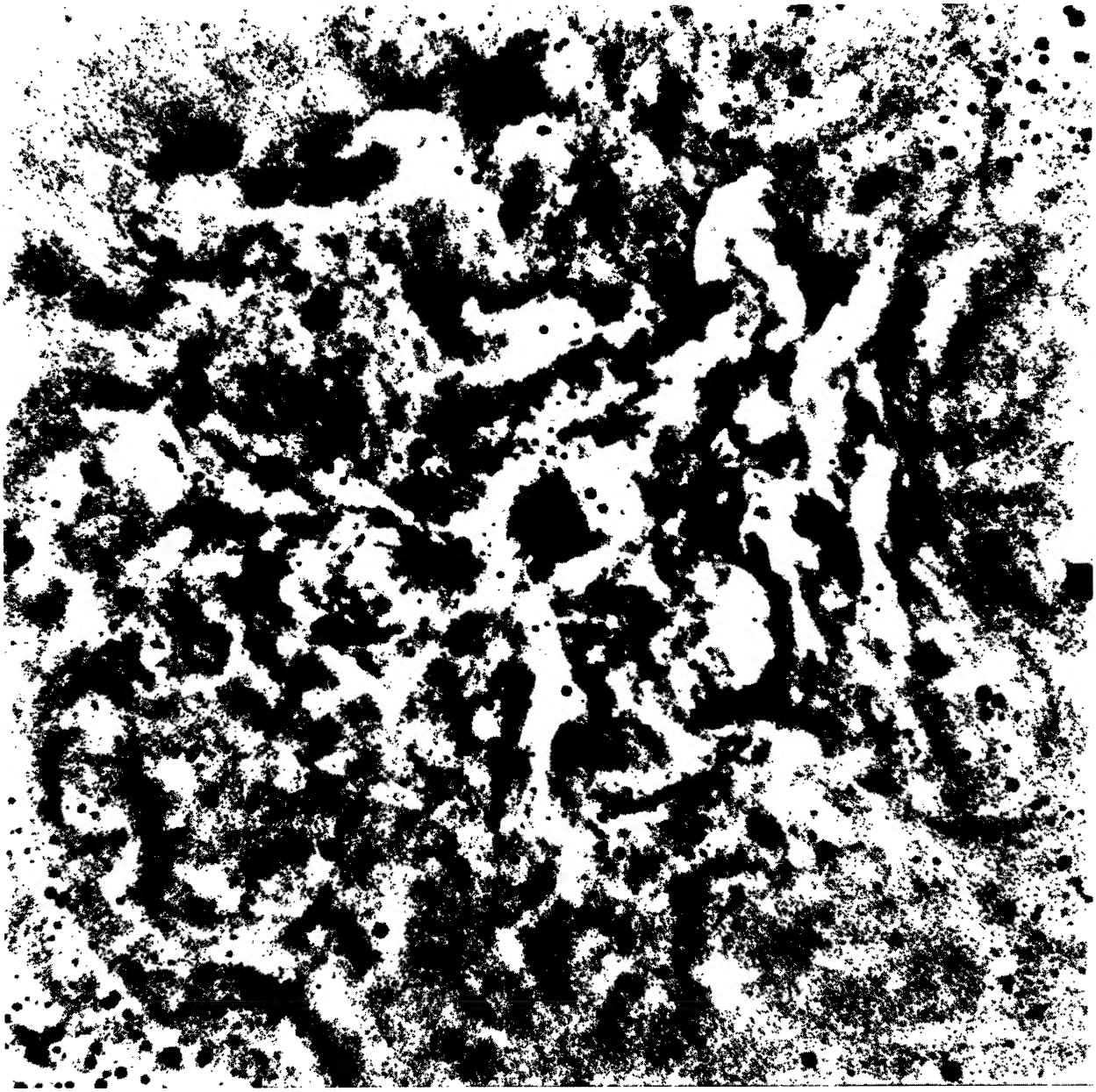

FIG. 2.—Ultraviolet image of the cluster area shows the extremely complex emission-reflection nebula. The area is 9'.71 on a side. North is at bottom, and east to the left.

FORTE AND ORSATTI (*see* page 212)

FIG. 18.—Blue output from SKYFLAT. A number of individual dark clouds can be recognized, mainly to the northwest of the central star. Orientation is the same as in Fig. 2.

FORTE AND ORSATTI (*see* page 228)

PLATE 6

FIG. 1*a*.—A short exposure, duPont telescope plate (CD 1010) of the edge-on galaxy NGC 4762. The inner bright part of the disk is extremely thin and is identified as a bar seen obliquely at an angle $\phi = 33° \pm 10°$ to the line of sight.

WAKAMATSU AND HAMABE (*see* page 283)

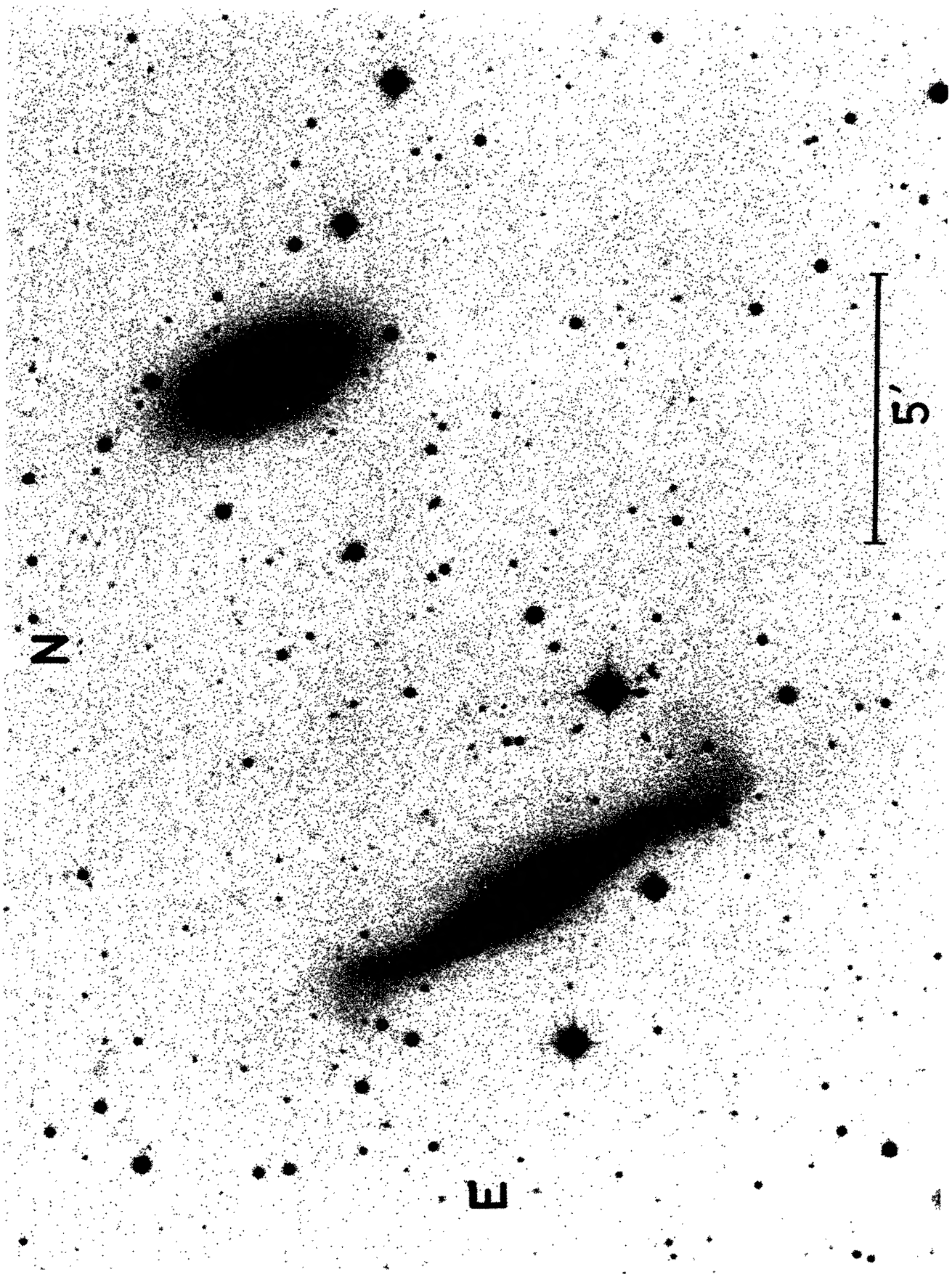

FIG. 1*b*.—A deep IIIa-J, Palomar Schmidt plate of the field NGC 4762. The faint outer envelope of NGC 4762 is identified as an outer warped ring. The bright SB(r)0$^-$: galaxy 10'.5 NW of NGC 4762 is NGC 4754.